

# Characterization of energy transfer processes occurring between pi-conjugated polymers and surface oxidized silicon nanoparticles

R. K. Ligman\*, L. Mangolini\*\*, U. R. Kortshagen\*\* and S. A. Campbell\*

\*Department of Electrical and Computer Engineering

\*\*Department of Mechanical Engineering

University of Minnesota, Minneapolis, MN, USA, campb001@umn.edu

## ABSTRACT

Electroluminescence (EL) from crystalline surface oxidized silicon nanoparticles (Si/SiO<sub>2</sub> nps) randomly dispersed within Poly(9-Vinyl Carbazole) (PVK) was obtained. The energy transfer processes between the PVK polymer host and Si/SiO<sub>2</sub> nps were investigated using intrinsic Poly(Fluorene)s (PFE). The PFE side chain lengths were selected to inhibit efficient energy transfer through direct carrier injection and Dexter processes by imposing a spatial separation between the polymer pi-conjugation and Si/SiO<sub>2</sub> nps. Scalar EL emission, with no contribution from the Si/SiO<sub>2</sub> nps, was observed from the three hybrid PFE(Si/SiO<sub>2</sub>) devices implying no direct carrier injection, Förster or Dexter energy transfer processes occur in the PFE hybrid devices. The Si/SiO<sub>2</sub> np loads used were well below the percolation threshold, verifying the observed bulk dominated JV characteristics, which strongly suggest the observed Si/SiO<sub>2</sub> np emission from the hybrid PVK device was produced by direct carrier injection.

**Keywords:** silicon nanoparticle, electroluminescence, hybrid device

## 1 INTRODUCTION

Since the discovery of size tunable visible emission from quantum confined porous Si nps, EL devices that utilize quantum efficient nps have been sought. Such devices have been fabricated by incorporating Si nps in different host matrices fabricated using cleanroom processing techniques.[1-6] These one step techniques are advantageous as they optimize the Si np quantum efficiency by inherently passivating dangling surface bonds with the host matrix. However, since the nps are embedded in insulating materials, most of the Si np EL is of low efficiency, generated by hot electrons at high energy expense. Due to the lack of suitable conductive host matrix materials that can survive the harsh temperatures and processing conditions required by these techniques it is preferred to utilize a three step process where (1) crystalline Si nps are fabricated, (2) passivated using ex-situ means and (3) incorporated into a conductive organic matrix. The non-thermal plasma fabrication technique developed by Mangolini et al. is well suited for this device fabrication technique as it mass produces highly crystalline Si nps with tight size control.[7] Ex-situ passivation by UV assisted photooxidation or hydrosilylation can be used to stabilize the Si np optical properties while tailoring the np surface chemistry.[8,9] Lastly, the pi-conjugated organic

matrix energy levels can be selected to construct thermodynamically favorable band alignments to complement the Si np band energies. A type I heterojunction is desirable for a device producing np emission. However, this band alignment means the observed np emission could be the result of direct carrier injection, excitons generated on the polymer and trapped by the nps (Förster or Dexter),[10,11] or from excitons generated by nps absorption of light emitted from the polymer (radiative).[12] As previously shown, a non-scalar emission dependence with the applied current density was observed from Si/SiO<sub>2</sub> nps dispersed in PVK and suggests that direct carrier injection is responsible for producing the observed Si np emission.[13] However, the coulombic interactions and strong overlap between the Si/SiO<sub>2</sub> np absorption and PVK emission imply energy transfer may also occur through Förster or Dexter processes.

In order to improve the device efficiency the energy transfer mechanisms between pi-conjugated polymers and Si/SiO<sub>2</sub> nps were investigated using intrinsic PFEs. PFEs are well suited for this study as they have a large bandgap, which straddles that of red-orange emitting Si/SiO<sub>2</sub> nps. The PFE side chain lengths were selected to inhibit efficient energy transfer through carrier injection and Dexter processes by imposing a spatial separation between the intrinsic polymer pi-conjugation and Si/SiO<sub>2</sub> nps. In such hybrid devices with a spatial separation less than 10Å Förster, Dexter and direct injection energy transfer may occur. For a spatial separation of more than 10Å the Förster process is permitted while the probability of the Dexter or direct injection processes decreases strongly with separation. The optical and electrical characterization of these devices is presented.

## 2 EXPERIMENTAL DETAILS

The Si nps used in this experiment were fabricated in a nonthermal plasma through the electron impact dissociation of silane gas, leading to cluster formation and nanocrystal growth, as described previously.[7] Downstream of the plasma, nanocrystals were collected in powder form on a stainless steel mesh. The Si np coated mesh was carefully transferred under nitrogen to chloroform (CHCl<sub>3</sub>) and ultrasonicated to create a nanoparticle dispersion of 0.1mg/ml. The as-produced nps did not photoluminesce (PL) due to incomplete surface passivation leaving non-radiative recombination centers. To improve the optical emission of the Si nps, a thin 1nm oxide shell was grown around the Si nps by ultra violet (UV) assisted photooxidation. The UV emission, centered at 365nm, photocleaves the Si np surface Si-H bonds creating activated Si surface sites that react with dissolved

oxygen in the  $\text{CHCl}_3$ . [8] Although the oxide shell is not ideal for all applications as it restricts the quantum confined bandgap from opening past  $\sim 2.1\text{eV}$ , [14] it produced stable properties for red emitting Si nps and is hence suitable for the purpose of demonstrating Si np EL. The Si/SiO<sub>2</sub> np PL, excited by a 365nm source, was measured using an OceanOptics USB2000 spectrometer and integrating sphere. The Si/SiO<sub>2</sub> np PL emission was centered at 650nm with a full width at half max of  $\sim 167\text{nm}$ .

Polymer(Si/SiO<sub>2</sub>) hybrid devices were fabricated by incorporating Si/SiO<sub>2</sub> nps in PVK, Poly(9,9-dihexylfluorenyl-2,7-diyl) end capped with DMP (PFH), Poly(9,9-dioctylfluorene-2,7-yleneethynylene) (PFE8) and Poly(9,9-didodecylfluorene-2,7-yleneethynylene) (PFD). PFH was purchased from HW Sands, PVK, PFE8 and PFD were purchased from SigmaAldrich. All materials were stored under nitrogen and used as received. The alkyl side chain lengths in increasing order are 8.696Å (PFH), 11.595Å (PFE8) and 17.393Å (PFD). Based on the side chain length and ignoring differences in exciton binding energy, PVK and PFH allow Förster, Dexter and direct carrier injection, while PFE8 and PFD allow Förster and inhibit Dexter and direct carrier injection. The host polymers were added at a concentration of 10mg/ml to 0.1mg/ml Si/SiO<sub>2</sub> np solution in  $\text{CHCl}_3$ . Control devices were fabricated as well. The polymer and polymer:Si/SiO<sub>2</sub> np  $\text{CHCl}_3$  solutions were spin cast onto clean ITO coated glass substrates producing 60nm thick films. The films were baked in a nitrogen environment at 100°C for 30 minutes to remove residual solvent. The top cathode, consisting of 80nm of Mg followed by 120nm of Ag was deposited through a shadow mask by thermal evaporation, producing 3.14mm<sup>2</sup> circles. The film quality and thickness was evaluated by tapping mode AFM. No phase segregation was observed in these films and all of the films were free of measurable pin holes, independent of the nanoparticle loading. These results imply that the Si/SiO<sub>2</sub> nps were well dispersed throughout the polymer matrices although a few aggregates may exist. [7]

### 3 RESULTS AND DISCUSSION

#### 3.1 PL and EL Emission

The PL emission from hybrid and control solutions were evaluated to ensure the Si/SiO<sub>2</sub> nps remained optically active when dispersed within the PVK and PFE polymers. The PL emission was measured from 1mL samples using a 365nm source, integrating sphere and spectrometer. Si/SiO<sub>2</sub> np PL emission was observed from all four solutions implying the nps remain optically active when dispersed in these polymers.

The EL emissions from PVK and PFE hybrid and control devices are shown in figure 1. The PVK hybrid device EL emission peaks at 415nm and 640nm correlate well with excimer emission from PVK and Si/SiO<sub>2</sub> np emission. [15,16] The strong 450nm peaks in the PFE emissions are from intrachain excitonic emission and the red shifted tails that diminish with increasing wavelength are from a ketone

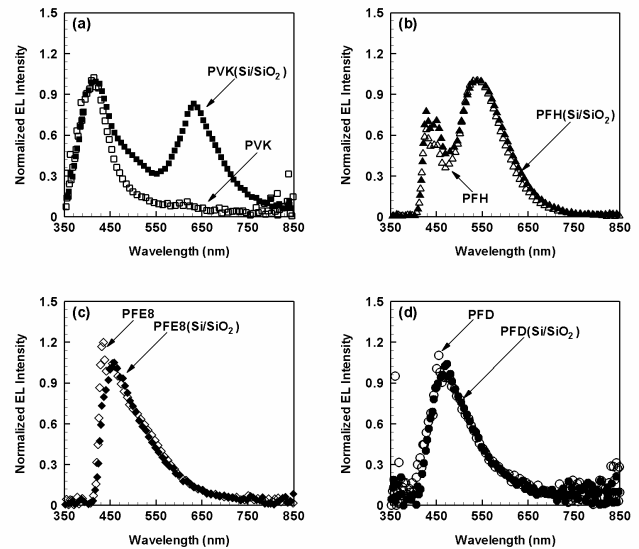


Figure 1: Normalized EL emission from hybrid and control devices.

defect. [17,18] There was no significant difference in the emission from hybrid and control devices of PFH, PFE8 and PFD. More importantly, there was no Si/SiO<sub>2</sub> np emission from the PFE hybrid devices.

The intensity of the polymer component in the hybrid EL emission was altered by the addition of the Si/SiO<sub>2</sub> nps to the polymer matrices. The polymer EL emission from hybrid devices compared to the control devices was reduced by a factor of 0.02 and 0.53 in PFH and PFE8 and increased by a factor of 7.1 and 21.2 in PFD and PVK matrices. In previous studies increased polymer emission was obtained by incorporating nps into the polymer host. [19] Within these devices the nps generate disorder that improves wavefunction localization and reduces non-radiative exciton loss. [20] The decreased emission observed from the PFH and PFE8 hybrid devices suggests an additional and at this time undetermined non-radiative mechanism exists by which carriers or excitons are lost within the device.

The hybrid device EL properties were characterized as a function of the applied current density and the results of this experiment are shown in figure 2. Simultaneous emission from the polymer and nps was observed from the extrinsic PVK(Si/SiO<sub>2</sub>) device where as polymer only emission was observed from the intrinsic PFH(Si/SiO<sub>2</sub>), PFE8(Si/SiO<sub>2</sub>) and PFD(Si/SiO<sub>2</sub>) devices. The normalized data revealed the emission from the PVK(Si/SiO<sub>2</sub>) device (see Fig. 2) was non-scalar with current density such that the 640nm Si/SiO<sub>2</sub> np emission increased with respect to the 415nm PVK emission. This shift is suggested to be the result of energy transferred from the PVK host to the Si/SiO<sub>2</sub> nps by direct carrier injection, Förster or Dexter mechanisms. The normalized PFH(Si/SiO<sub>2</sub>), PFE8(Si/SiO<sub>2</sub>) and PFD(Si/SiO<sub>2</sub>) emission (see Fig. 2) were scalar with increasing current density therefore confirming no energy transfer occurred between the intrinsic polymers and Si/SiO<sub>2</sub> nps. The independence of the observed scalar emission from the PFE hybrid devices on the

side chain length suggests that the observed Si/SiO<sub>2</sub> np emission from the PVK(Si/SiO<sub>2</sub>) device may be the result of direct carrier injection. Measurements of the polymer and Si/SiO<sub>2</sub> np exciton binding energies and recombination rates will be collected to verify these results.

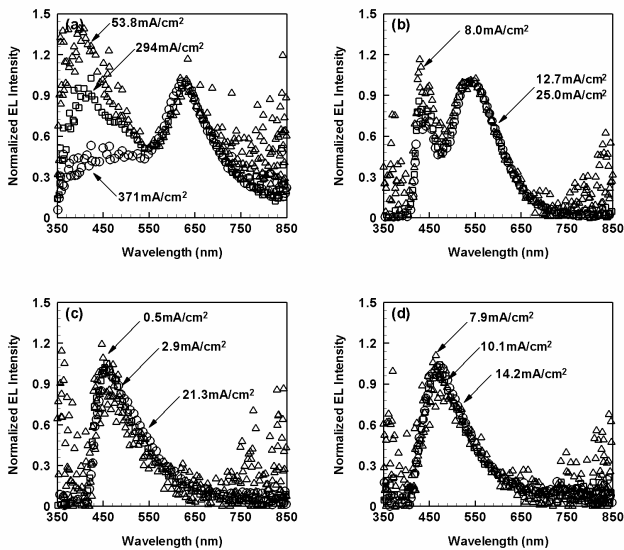


Figure 2: Normalized hybrid device EL emission with current density. (a) PVK(Si/SiO<sub>2</sub>), (b) PFH(Si/SiO<sub>2</sub>), (c) PFE8(Si/SiO<sub>2</sub>) and (d) PFD(Si/SiO<sub>2</sub>).

### 3.2 EL Quantum Efficiency

The relative EL quantum efficiency (QE) with applied power of the hybrid and control devices was measured. The light emitted perpendicular from the devices was collected and no corrections were performed to account for the substantial amount of light channeled through the sides of the glass substrate. Therefore, only the relative efficiencies can be quoted. As shown in figure 3, the hybrid and control device

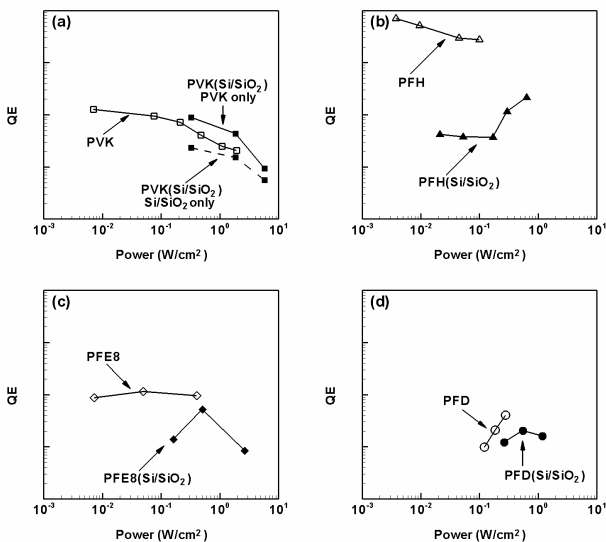


Figure 3: Relative hybrid and control device QE with applied power. Lines are guides to the eye.

QEs roll off with increased applied power as observed with hybrid devices investigated by other groups. The QE for all hybrid devices was lower than the control device QE. The reduced QE with the introduction of nps is in part due to the increased current density supported by the hybrid films and may also be in part due to an additional non-radiative decay mechanism introduced by the Si/SiO<sub>2</sub> nps.

### 3.3 Current-Voltage Response

The transient current-voltage response of the hybrid and control devices were evaluated and the results shown in figure 4. All devices showed rectifying behavior with no light emission under reverse bias as expected. Furthermore, two distinct operating regions exist for these devices. At low fields the current is roughly proportional to the square of the voltage, agreeing with the classic space charge limited conduction (SCLC) model for an ideal material.[21] At high fields the device response followed strong SCLC with an exponential distribution of traps, characterized by  $J \propto V^m$ .

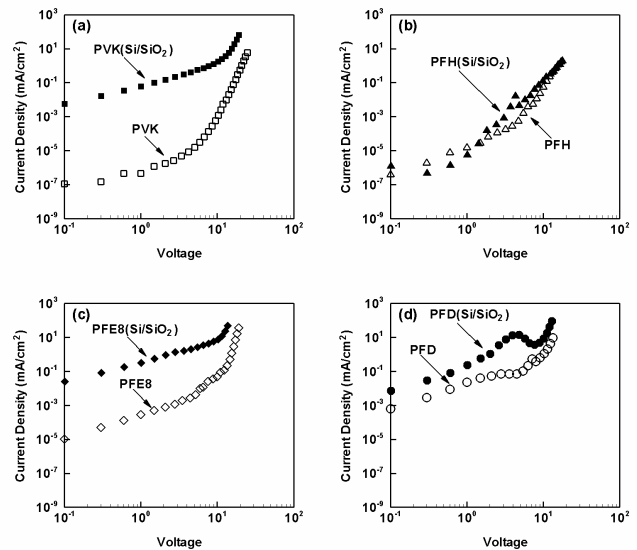


Figure 4: Transient device current-voltage response.

The device current-voltage response with Si/SiO<sub>2</sub> np loading of 0%, 0.1%, 0.5%, and 1.0% were investigated in PVK and PFE8 matrices. The values of the exponent  $m$  within the strong SCLC regime varied independently of the Si/SiO<sub>2</sub> loading in both PVK and PFE8 verifying the nps did not significantly alter the carrier transport mechanisms within these devices. This was expected since the np loads used are well below the percolation threshold. The PFH hybrid device current-voltage response (see Fig. 4) and drive voltage (see Fig. 5) agree well with the PFH control device supporting that the device carrier transport properties are dominated by the polymer host. However, PVK, PFE8 and PFD hybrid devices showed significant differences such as increased current density with voltage (see Fig. 4) and a 3 to 8V reduction in drive voltage (see Fig. 5). The decreased drive voltage and increased current density suggests the Si/SiO<sub>2</sub> nps indirectly affect the carrier transport properties of the bulk polymer

film, perhaps by behaving as carrier traps. The observed current-voltage response of the PVK and alkyne-bridged PFE8 and PFD polymers agree with published results from other groups.[19]

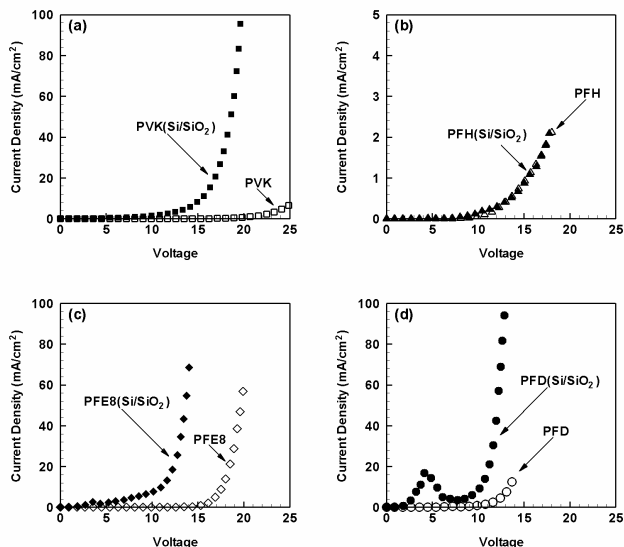


Figure 5: Hybrid and control device drive voltage.

## 4 CONCLUSIONS

The energy transfer processes in hybrid devices based on Si/SiO<sub>2</sub> nps dispersed in PVK and PFE polymers were investigated using spatial separation. The PFE side chains were selected to impose a known spatial separation of 8.696Å (PFH), 11.595Å (PFE8) and 17.393Å (PFD) between the polymer pi-conjugation and Si/SiO<sub>2</sub> nps. Since no measurable Si/SiO<sub>2</sub> np emission was observed from the PFE hybrid devices it is implied that for the specified devices no direct carrier injection, Förster, or Dexter energy transfer occurs between the intrinsic PFE polymers and Si/SiO<sub>2</sub> nps. The PVK and PFE8 hybrid device current-voltage responses and drive voltages were bulk dominated, independent of the Si/SiO<sub>2</sub> np loading. These findings confirm that the PVK host polymer was directly involved in the carrier transport mechanism resulting in the observed Si/SiO<sub>2</sub> np emission. However, the Si/SiO<sub>2</sub> nps indirectly affected the carrier transport properties in PVK, PFE8 and PFD by increasing the current density with voltage response and decreasing the device drive voltages. Further experiments regarding the polymer exciton binding energies and recombination rates will be collected to verify the observed results.

## 5 ACKNOWLEDGEMENTS

This work was supported in parts by NSF under MRSEC grant DMR-0212302, and grant CMMI-0556163. Partial support was also provided by SPAWAR. This work was performed at the Minnesota NanoFabrication Center and which receives support from the NSF through NNIN.

## REFERENCES

- [1] O. Jambios, H. Rinnert, X. Devaux and M. Vergnat, *J. Appl. Phys.* 98, 046105, 2005.
- [2] C. Lui, C. Li, A. Ji, L. Ma, Y. Wang and Z. Cao, *Appl. Phys. Lett.* 86, 223111, 2005.
- [3] S. Hazra, I. Sakata, M. Yamanaka and E. Suzuki, *J. Appl. Phys.* 96, 7532, 2004.
- [4] P. Photopoulos and A. Nassiopoloulou, *Appl. Phys. Lett.* 77, 1816, 2000.
- [5] T. Kim, N. Park, K. Kim, G. Sung, Y. Ok, T. Seong and C. Choi, *Appl. Phys. Lett.* 85, 5355, 2004.
- [6] S. Thompson, C. Perrey, C. Carter, T. Belich, J. Kakalios and U. Kortshagen, *J. Appl. Phys.* 97, 034310, 2005.
- [7] L. Mangolini, E. Thimsen and U. Kortshagen, *Nano Lett.* 5, 655, 2005.
- [8] R. Cicero, M. Linford and C. Chidsey, *Langmuir* 16, 5688, 2000.
- [9] F. Hua, M. Swihart and E. Ruckenstein, *Langmuir* 21, 6054, 2005.
- [10] S. Hong and K. Yeon, *J. Korean Phys. Soc.* 45, 1568, 2004.
- [11] F. Pschenitzka and J. C. Sturm, *Appl. Phys. Lett.* 79, 4354, 2001.
- [12] D. Kovalev, J. Diener, H. Heckler, G. Polisski, N. Künzner and F. Koch, *Phys. Rev. B* 61, 4485, 2000.
- [13] R. K. Ligman, L. Mangolini, U. R. Kortshagen and S. A. Campbell, *Appl. Phys. Lett.* 90, 061116, 2007.
- [14] M. Wolkin, J. Jorne, P. Fauchet, G. Allan and C. Delerue, *Phys. Rev. Lett.* 82, 197, 1999.
- [15] W. Klöpffer, *Chem. Phys. Lett.* 4, 193, 1969.
- [16] Y. Nozue, T. Hisamune, T. Goto and H. Tsuruta, *J. Phys. Soc. Jpn.* 52, 2983, 1983.
- [17] J. M. Lupton, M. R. Craig and E. W. Meijer, *Appl. Phys. Lett.* 80, 4489, 2002.
- [18] J. M. Lupton, P. Schouwink, P. E. Keivanidis, A. C. Grimsdale and K. Müllen, *Adv. Funct. Mater.* 13, 154, 2003.
- [19] J. Park, S. Kim, Y. Kim and O. Park, *Nanotech.* 16, 1793, 2005.
- [20] J. Brédas, J. Cornil and A. J. Heeger, *Adv. Mat.* 8, 447, 1996.
- [21] N. Mott and R. Gurney, "Electronic processes in ionic crystals", Oxford University Press London, 168, 1940.